

# Polyaniline/akaganéite nanocomposite for detoxification of noxious Cr(VI) from aquatic environment

Shaker Ebrahim<sup>1</sup> · Azza Shokry<sup>2</sup> · Hesham Ibrahim<sup>2</sup> · Moataz Soliman<sup>1</sup>

Received: 19 November 2015 / Accepted: 22 March 2016 / Published online: 29 March 2016  
© Springer Science+Business Media Dordrecht 2016

**Abstract** In this work, a removal of toxic hexavalent chromium Cr(VI) ion from aqueous solution was investigated and studied using nanocomposite of polyaniline (PANI) and akaganéite nanoparticles (NP). HCl doped PANI, and akaganéite NPs were prepared by chemical oxidative polymerization and co-precipitation techniques, respectively. The synthesized materials were characterized by Fourier transform infrared spectroscopy (FTIR), X-ray diffraction (XRD), scanning electron microscope (SEM), and high-resolution transmission electron microscope (HRTEM). It was indicated that the formed oxide NPs were consisted of akaganéite as dominant phase plus minor phases of hematite, magnetite, and/or maghemite. HRTEM images of the prepared nanocomposite demonstrated that the phases of oxide NPs embedded in the nanocomposite had the same crystallinity and morphology of pristine oxide NPs. It was found that size of nanocomposite particles has diameter ranged from 8.95 to 16.21 nm. Cr(VI) removals in a wide pH range from 2 to 9 were appropriated for prepared nanocomposite. The nanocomposite has demonstrated high removal percentage of 99.2 % and removal capacity of 17.36 mg/g for 7.0 mg/L Cr(VI) polluted aqueous solution at pH 2.0 for 5-min contact time. The synthesized nanocomposite was applied to remove Cr(VI) from a leather tanning wastewater sample with efficiency of 93.4 %.

**Keywords** Polyaniline · Chromium · Akaganéite · Nanocomposite · Magnetite · Metal Oxide · Nanoparticles

## Introduction

Today's world faces challenge in the rising demand for clean drinking water, and the water scarcity in terms of both quantity and quality has become a significant threat to the well-being of humanity. The waste products from industrial activities are mainly responsible for contaminating the water. This contaminated water contains heavy metal ions such as arsenic, zinc, copper, nickel, mercury, cadmium, lead, and chromium that are carcinogenic to human beings and harmful to the environment. Therefore, it is important to remove these heavy metals from water and wastewater. Among the heavy metals, hexavalent chromium (Cr(VI)) is being one of the most heavy metal pollutants in the environment. This metal is released to from various industries like mining, electroplating, leather tanneries, paints, pigments, and chrome manufacturing industries. The permissible limit of Cr(VI) for industrial effluents to be discharged to the surface water is 0.1 mg/L while for potable water is 0.05 mg/L according to the World Health Organization [1].

Conventional methods for detoxification the heavy metals from aqueous solutions include the following: adsorption, chemical precipitation, ion exchange, electro dialysis, and membrane filtration [2]. The drawbacks associated with precipitation method are large consumption of reagents and high volume of sludge generation. Ion exchange, membrane processes, and electro dialysis are cost-effective methods. On the other hand, adsorption method is efficient technique for removing toxic heavy metals from water because of its low cost and high efficiency. Besides, adsorption can effectively remove heavy metals from the wastewater at

✉ Shaker Ebrahim  
shebrahim@alex-igsr.edu.eg

<sup>1</sup> Department of Materials Science, Institute of Graduate Studies and Research, Alexandria University, PO Box 832, 163 Horreya Avenue, El-Shatby, Alexandria, Egypt

<sup>2</sup> Department of Environmental Studies, Institute of Graduate Studies and Research, Alexandria University, PO Box 832 Alexandria, Egypt

low concentrations. Consequently, numerous adsorbents have been developed for the removal of such hazardous metals from wastewater [3].

The conducting polymers based on aromatic or heterocyclic monomers like aniline, pyrrole, thiophene, and their derivatives have been attracted a great attention in recent years due to their good environmental stability. Polyaniline (PANI) is now regarded as one of the most technologically promising electrically conductive polymers due to its ease of synthesis, low cost, high yield, and relatively stable electrical conductivity [4]. PANI has been reported as being used for heavy metals removal. PANI powder has rough surface and looks like good candidate for heavy metals removal due to the interesting properties such as special doping mechanisms, large specific surface area, high environmental stability, nontoxicity, low cost, and easy bulk production. It also shows great potential for applications such as light-emitting diodes, chemical sensors, and electronic devices [5, 6].

A variety of efficient, cost-effective, and environmentally friendly nanomaterials have been developed, each possessing a unique functionality in their potential application to the detoxification of water/wastewater. Among the various kinds of nano-adsorbents, metal oxide nanoparticles play an important role in water/wastewater purification. There have been several reports on iron oxides such as hematite ( $\alpha$ - $\text{Fe}_2\text{O}_3$ ), akaganéite ( $\beta$ - $\text{FeOOH}$ ), and magnetite ( $\text{Fe}_3\text{O}_4$ ) being used as nano-adsorbents for the removal of various toxic metal ions from wastewater [7–9]. These oxide phases nano-adsorbents are effective and economical for the rapid removal and recovery of metal ions from wastewater effluents due to their large surface area and magnetic properties. They can be reused after magnetic separation in removing the toxic metal ions. However, most of these nanomaterials are prone to agglomeration, and their high capacity and selectivity would be greatly decreased. One of the most effective ways in solving these problems is to incorporate these nano-oxides into polymeric matrices. In addition, the incorporation of these nanoparticles into polymeric materials enhances the physical properties of these polymers.

Recently, a great effort has been devoted to combine PANI with  $\text{Fe}_3\text{O}_4$  to form nanocomposite adsorbents using different preparation techniques for Cr(VI) ions. Gu et al. [10] prepared magnetic PANI/ $\text{Fe}_3\text{O}_4$  nanocomposites using surface-initiated polymerization method for the removal of Cr(VI) from aqueous solutions. They reported that a complete Cr(VI) removal from 20.0 ml neutral solution with an initial Cr(VI) concentration of 1.0–3.0 mg/L after 5-min treatment period with nanocomposites load of 10 mg was found. Han et al. [11] synthesized PANI/ $\text{Fe}_3\text{O}_4$  microspheres through an interfacial polymerization approach for Cr(VI) removal from water, and they found that a strong adsorption capacity of 200 mg/g was obtained. Li et al. [12] prepared magnetic  $\text{Fe}_3\text{O}_4$  and PANI nanocomposite for reduction of Cr(VI) to low toxic Cr(III)

ions, and the results showed that a concentration of Cr(VI) solutions (10 mg/L, 50 ml) can be ( $\geq 99\%$ ) reduced by the nanocomposite (0.01 g). Rezvani et al. [13] prepared PANI/ $\text{Fe}_3\text{O}_4$  nanocomposite by oxidative polymerization of aniline in the presence of  $\text{Fe}_3\text{O}_4$  nanoparticles for the preconcentration of Cr(VI) anions from spiked water samples, and the results showed that sorption capacity of the sorbent for Cr(VI) was 54 mg/g. Tang et al. [2] synthesized magnetic mesoporous silica composite with PANI grafted for Cr(VI) removal from aqueous solution, and the maximum Cr(VI) removal efficiency was nearly 95 % at pH 2.0.

Akaganéite is  $\text{Fe}^{3+}$  oxide-hydroxide ( $\beta$ - $\text{FeOOH}$ ) and has a monoclinic crystal system with a brownish yellow streak. The akaganéite structure has an iron oxyhydroxide framework containing tunnels partially filled with chloride anions in chloride-containing environments. This tunnel structure makes akaganéite an especially interesting material in many areas of applications, such as electrode material, catalyst, ion exchange material, and adsorbent. Akaganéite is usually prepared by the hydrolysis of  $\text{FeCl}_3$  aqueous solutions at moderate temperatures. Nanocrystalline akaganéite has high surface areas, narrow pore size distribution with different crystal shapes. Because of its unique properties, it has been widely used as an adsorbent to remove contaminants from water and liquid hazardous wastes [14]. The main objective of this work is to study the effect of akaganéite phase on the physical properties of doped PANI to prepare nanocomposite material for detoxification of noxious hexavalent chromium (Cr(VI) ions from aqueous solution. PANI doped with HCl, and akaganéite NPs were prepared by chemical oxidative polymerization and co-precipitation techniques, respectively. Finally, PANI and akaganéite NPs were characterized by Fourier transform infrared (FTIR), X-ray diffraction (XRD), scanning electron microscope (SEM), and high-resolution transmission electron microscope (HRTEM) techniques.

## Materials and methods

### Materials

Aniline monomer (98.5 %), ammonia solution (33.0 %), and ortho-phosphoric acid (85wt %) were obtained from El Nasr Chemical Company. Hydrochloric acid (36.0 %), acetone (99.5 %), and sodium hydroxide (98.0 %) were purchased from Sigma-Aldrich. Potassium dichromate (99.0 %) was received from Merck. Ammonium persulfate (APS) (98.0 %), methanol (HPLC grade), and ethanol (HPLC grade) were obtained from Fisher Scientific, UK. Anhydrous ferrous chloride (99.0 %), anhydrous ferric chloride (98.0 %), and 1, 5-diphenylcarbazine (DPC) (98.0 %) were obtained from Across Organics, USA.

### Synthesis of akaganéite nanoparticles

Akaganéite nanoparticles (NPs) were synthesized by coprecipitation of  $\text{Fe}^{2+}$  and  $\text{Fe}^{3+}$  ions in the presence of alkaline solution. Anhydrous ferrous chloride (3.121 g) and anhydrous ferric chloride (1.275 g) were dissolved in 25 ml hydrochloric acid (0.4 M). This mixture was added drop-wise into 250 ml sodium hydroxide solution (1.5 M) placed in a three-necked flask with vigorous stirring under nitrogen gas. The obtained dark brown precipitate was heated at 75 °C for 30 min. The precipitate was collected through a powerful magnet, washed sequentially with distilled water and ethanol. The dark brown colored powder of akaganéite NPs was obtained upon drying at room temperature.

### Synthesis of polyaniline

The chemical oxidative polymerization of aniline to obtain emeraldine salt was carried out in an aqueous acidic solution. Ammonium persulphate (27 g) was dissolved in hydrochloric acid (1 M) and cooled to 0 °C. Aniline (40 ml) was also dissolved in pre-cooled hydrochloric acid (1 M). Acidic solution of the ammonium persulphate was then slowly added to aniline solution to prevent the temperature from exceeding 5 °C. The mixture was left for 24 h with continuous stirring using a magnetic stirring bar at 5 °C (ice bath) to ensure the completion of polymerization. The green powder of polyaniline hydrochloride (PANI-ES) was collected on a filter paper using vacuum pump and washed consecutively with distilled water, methanol, and acetone until filtrate became colorless, then dried at room temperature.

### Synthesis of PANI/akaganéite nanocomposite

PANI/akaganéite nanocomposite (NC) was prepared by a mechanical mixed of each akaganéite nanoparticles and PANI separately and then amounts of PANI (70 wt %) and akaganéite NPs (30 wt%) were physically mixed by grinding in a mortar.

### Characterization techniques

The morphology of the products was characterized by SEM (SEM "JEOL JSM-5300"). Samples were used in the powder form and were coated with sputtered gold layer. Also the morphology and particles size were investigated using HRTEM (JEM-2100 with selected area electron diffraction capability SAED). HTTEM sample was prepared by dispersing 2 mg of powder sample in 5 ml of ethanol and sonicated. A drop of this colloidal solution was evaporated on a copper grid and tested. The crystalline structures of the samples were evaluated by XRD analysis using (X-ray 7000 Shimadzu-Japan) at room temperature. The X-ray source was Cu target generated at

30 KV and 30 mA with scan speed 4 deg  $\text{min}^{-1}$ . FTIR spectrophotometer (Spectrum BX 11- LX 18–5255 Perkin Elmer) was used for measuring the IR spectra of the prepared samples. The samples were milled with dry potassium bromide at room temperature. The spectrum was recorded in the wavenumber range of 4000–350  $\text{cm}^{-1}$ . The thermogravimetric analysis (TGA) and differential scanning calorimetry (DSC) of the NC were conducted before and after treatment with Cr(VI) to determine their thermal stability using (TA instruments, STD Q—600) with a heating rate of 10 °C  $\text{min}^{-1}$  under  $\text{N}_2$  flow rate of 100  $\text{ml min}^{-1}$  from 21 °C to 400 °C.

### Measurements of removal percentage and capacity of Cr(VI) using PANI/akaganéite nanocomposite

Stock solution of 500 mg/L of Cr(VI) was prepared by dissolving potassium dichromate in deionized water. Cr (VI) solutions with the required concentration were freshly diluted from the stock solution. Batch experiments were carried out by mixing 10.0 mg (equivalent to 0.4 g/L) of NC with 25 ml of Cr(VI) aqueous solutions. These mixtures were stirred under sonication for a fixed time of 6 min. Adsorbent NC was separated from the pollutant solutions by using a magnet bar. Then, these solutions were filtered through filter paper of Whatman no.5, and the clear filtrates were analyzed for residual amount of Cr(VI) by colorimetric method [3].

The absorbance of the samples was measured using UV-VIS spectrophotometer (Evolution 300 UV-visible spectrophotometer, Thermo scientific, USA) at a fixed wavelength of 540 nm. The potential application for removal of Cr(VI) ions by NC from wastewater sample was also studied. The pH of Cr(VI) solutions was adjusted by NaOH (1 M) and HCl (1 M) with a pH meter (Martini MI150 pH/temperature Bench Meter). The NC (0.4 g/L) was ultrasonically dispersed in 25 ml Cr(VI) solutions (7 mg/L) for 6 min.

An industrial wastewater sample was collected from effluent of a leather tanning company in Alexandria, Egypt, contaminated with 0.6 mg/L and spiked with 6.0 mg/L to have 6.6 mg/L of Cr(VI) ions is selected to accomplish this study. The spiked wastewater sample was studied for the removal of Cr(VI) ions by mixing 25 ml of this sample with 0.4 g/L of NC pH 2.0 and pH 7.2 (the pH of the wastewater sample was 7.2) for 6 min. All removal experiments were carried out at room temperature. The removal percentage ( $R$ , %) and capacity ( $Q$ , mg/g) of Cr (VI) were calculated using the following equations:

$$R = \frac{C_0 - C_e}{C_0} \times 100 \quad (1)$$

where  $C_0$  and  $C_e$  are the initial and final Cr(VI) concentration (mg/L), respectively.

$$Q = \frac{C_0 - C_e}{m} \times V \quad (2)$$

where  $V$  represents the volume of Cr(VI) solution (ml), and  $m$  is the adsorbent mass (mg).

## Results and discussion

### Structural property of PANI/akaganéite nanocomposite

The FTIR spectroscopy is a powerful tool for analyzing the molecular structure of the prepared materials. FTIR spectrum of PANI presented in Fig. 1 indicates the characteristic bands of doped PANI. The band at  $1118 \text{ cm}^{-1}$  is attributed to the vibration of the  $-\text{NH}^+$  structure formed in the acid doping process of polyaniline [15]. Bands at  $1434$  and at  $1638 \text{ cm}^{-1}$  are assigned to the stretching of the benzenoid ring and quinoid ring [16]. The band at  $3458 \text{ cm}^{-1}$  represents the N-H stretching mode [17]. FTIR spectrum of the prepared akaganéite shown in Fig. 1 presents the characteristic peak at  $590 \text{ cm}^{-1}$  that attributes to the Fe-O stretching band of iron-oxide NPs [7, 10]. The absorption bands at  $1646 \text{ cm}^{-1}$  and at  $3430 \text{ cm}^{-1}$  are due to bending and stretching vibrations of O-H bonds in surface water molecules [18]. FTIR spectrum of NC shown in Fig. 1 appears the absorption peaks of PANI. In addition, the absorption peak at  $618 \text{ cm}^{-1}$  is attributed to the vibration of Fe-O band in iron-oxide NPs and has a peak shift from  $590 \text{ cm}^{-1}$  (in the pure iron-oxide nanoparticles) to  $618 \text{ cm}^{-1}$  (in the NC). This result indicates that the NC is successfully synthesized, and the observed shift indicates the interaction between PANI and akaganéite NPs [19]. To further understand the interaction mechanism between NC and Cr(VI), the FTIR spectra of the samples before and after Cr(VI) adsorption were recorded, as shown in Fig. 1. The absorption peak of quinoid ring at  $1580 \text{ cm}^{-1}$  and the peak of benzenoid ring at  $1480 \text{ cm}^{-1}$  in NC after Cr(VI) adsorption become more intense than that of the pristine NC. This is indicating that some emeraldine salts form convert to the pernigraniline form (the complete oxidation of PANI) [20]. These two bands in the treated NC have shifted to lower frequency compared with those of untreated NC confirming the Cr(VI) adsorption by PANI of the NC. In addition, the band at  $618 \text{ cm}^{-1}$  corresponds to Fe-O stretching bond in untreated NC has shifted to  $578 \text{ cm}^{-1}$  proving the adsorption of Cr(VI) on the iron oxide surface [7].

### Crystalline property of PANI/akaganéite nanocomposite

X-ray diffraction is a powerful technique used to identify the phases (crystalline or amorphous) in the material. The crystallinity of PANI, iron-oxide NPs, and NC was investigated as shown in Fig. 2. The PANI diffractogram presents two peaks

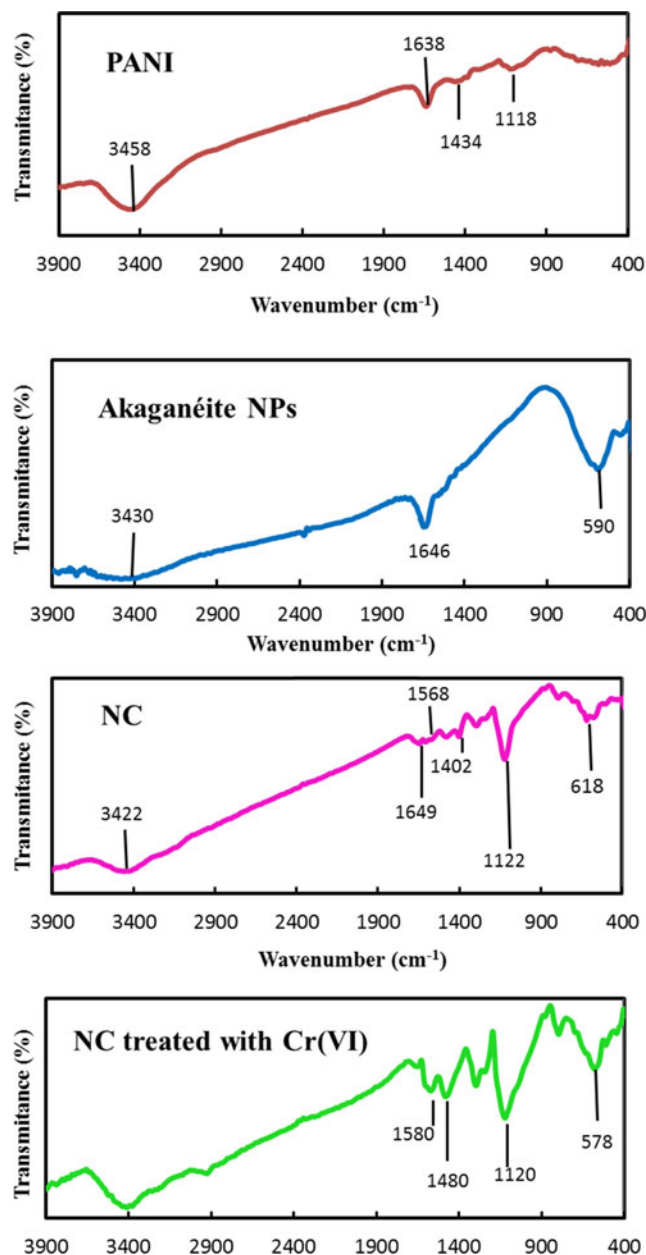


**Fig. 1** FTIR spectra of PANI, akaganéite NPs, NC, and NC treated with Cr(VI)

of PANI at  $2\theta = 12^\circ$  and  $25^\circ$  corresponding to (011) and (200), respectively. The strong peak at  $25^\circ$  indicates that PANI is a partially crystalline polymer. The partial crystallinity of PANI may be due to the amine and imine groups in the structure of PANI which can form stronger intermolecular and intramolecular hydrogen bonds [17]. The broad diffraction peak occurred between  $2\theta = 6^\circ$  and  $30^\circ$  is also due to the periodicity of the crystallographic planes that are parallel and perpendicular to the doped PANI chains and presence of an amorphous state in PANI [21]. XRD pattern of the iron-oxide NPs shows the characteristic peaks for akaganéite ( $\beta\text{-FeOOH}$ ) at  $2\theta = 12.3^\circ$  and at  $27.2^\circ$  which can be indexed to (110) and (310),

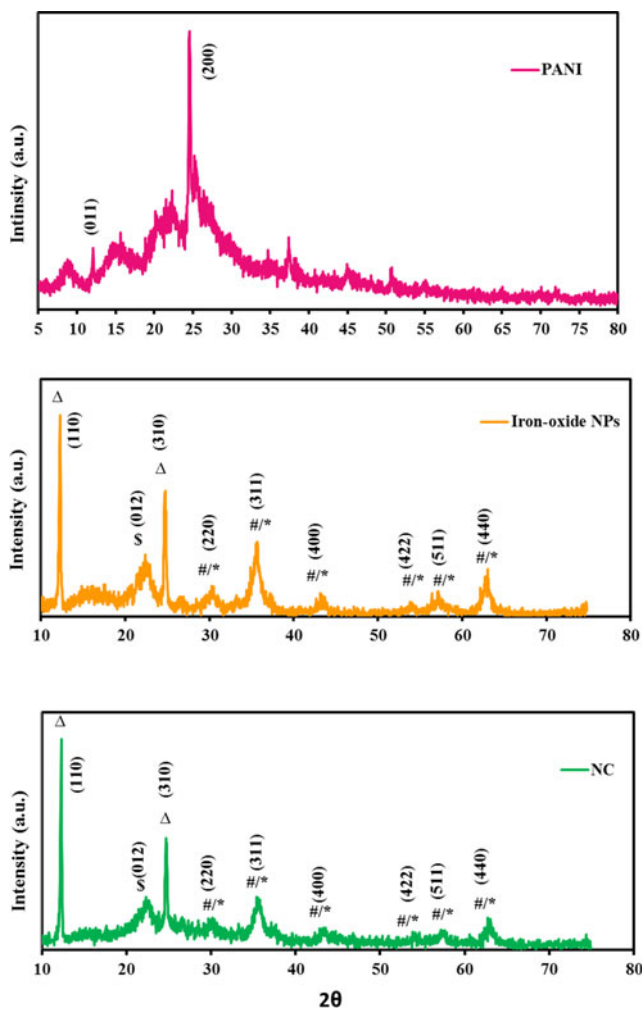


**Fig. 2** XRD patterns of PANI, iron-oxide NPs and NC. *Triangle*  $\beta$ -FeOOH, *dollar sign*  $\alpha$ -Fe<sub>2</sub>O<sub>3</sub>, *number sign* Fe<sub>3</sub>O<sub>4</sub>, and *asterisk*  $\gamma$ -Fe<sub>2</sub>O<sub>3</sub>

respectively (Joint Committee on Powder Diffraction Standards (JCPDS) No. 34–1266), hematite ( $\alpha$ -Fe<sub>2</sub>O<sub>3</sub>) at  $2\theta = 24.7^\circ$  corresponding to (012) (JCPDS No. 89–0597), plus six peaks for magnetite (Fe<sub>3</sub>O<sub>4</sub>) or maghemite ( $\gamma$ -Fe<sub>2</sub>O<sub>3</sub>) at  $2\theta = 30.1^\circ, 35.5^\circ, 43.1^\circ, 54^\circ, 57.0^\circ$ , and at

$62.6^\circ$ , marked by their indices of (220), (311), (400), (422), (511), and (440), respectively (JCPDS No. 85–1436). These results indicate that iron-oxide NPs consist of a complex mixture of akaganéite which is the main component in the prepared iron-oxide NPs, plus hematite, magnetite, and/or maghemite phases. The phase identification of magnetite and maghemite by the conventional XRD method is not simple because both of them have the same cubic structure, and their lattice parameters are almost identical. X-ray data of NC presents crystalline peaks almost similar to those obtained from the pure iron-oxide NPs revealing that no additional crystalline order introduced into the nanocomposite. This result reveals that there is an iron-oxide NPs layer coated on the surface of the PANI.

### Morphological property of PANI/akaganéite nanocomposite

The SEM images of PANI, akaganéite NPs and NC are shown in Fig. 3. The morphology of PANI indicates that the synthesized PANI consists of sponge structure and granular particulates. SEM micrograph of akaganéite NPs shows the formation of agglomerated particles due to magnetic dipole-dipole interactions between the particles [19, 22]. SEM image of NC presents a layer of akaganéite NPs coated on the surface of the PANI flake (dark color represents the akaganéite NPs and white color represents PANI). In addition, the morphological investigations of PANI, akaganéite NPs, and NC using HRTEM at different magnifications as shown in Fig. 4 demonstrate that PANI particles are nearly sheets of spherical shaped with presence of some agglomerations, and their diameter is ranged from 15.88 to 18.02 nm. HRTEM images of akaganéite NPs reveal that akaganéite NPs composed of large number of aggregated particles with nearly quasi-cube shape with particles diameter ranged from 6.62 to 10.41 nm. The interplanar spaces are clearly shown indicating high crystalline materials, which was confirmed by the selected area

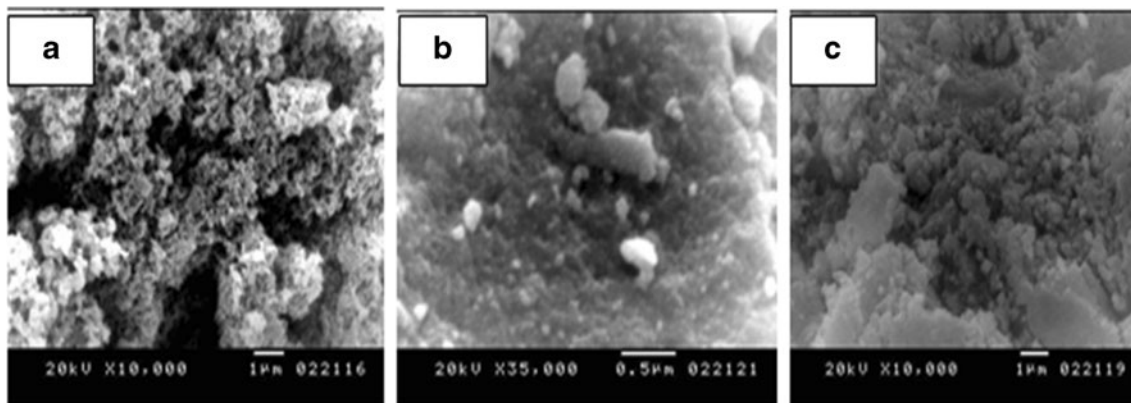


**Fig. 3** SEM images of PANI (a), akaganéite NPs (b), and NC(c)

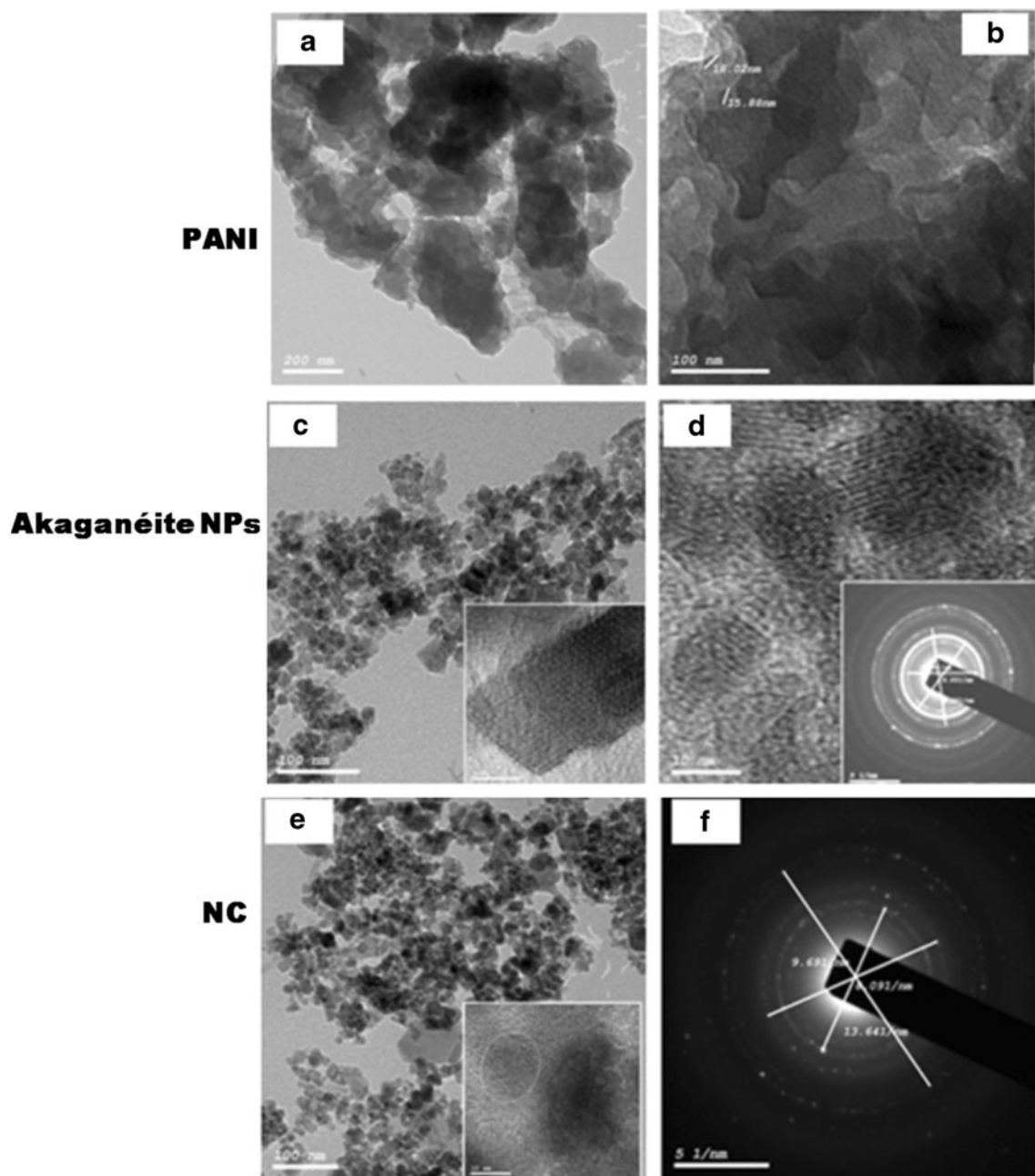


**Fig. 4** HRTEM images of PANI, akaganéite NPs and NC and their SAED

electron diffraction (SAED) pattern in the inset to the HRTEM images. The inset in Fig. 4c, d shows the existence of well-resolved lattice fringes of akaganéite NPs indicating that akaganéite NPs have nanocrystal structure. The electron diffraction pattern of akaganéite NPs inset in Fig. 4d indicates the polycrystallinity of the nanoparticles with an average d-spacing of 1.39 nm. HRTEM images of NC at different magnifications demonstrate that akaganéite NPs exist in the nanocomposite with the same morphology of pristine iron-oxide NPs. It is noted that size of NC particles is in the nanoscale, and the particles diameter ranged from 8.95 to 16.21 nm. In addition, the

inset of Fig. 4e depicts the lattice space of single crystal of NC. The electron diffraction pattern in Fig. 4f shows that NC is a polycrystalline material with an average d-spacing of 2.78 nm.

#### Thermal analysis of PANI/akaganéite nanocomposite

The TGA and DSC of NC were carried out before and after treated with Cr(VI) to study their thermal stability. Figure 5 shows TGA and DSC curves of untreated NC and treated NC with Cr(VI). The weight loss from room temperature to  $\sim 134$  °C for untreated NC and to  $\sim 136$  °C for NC

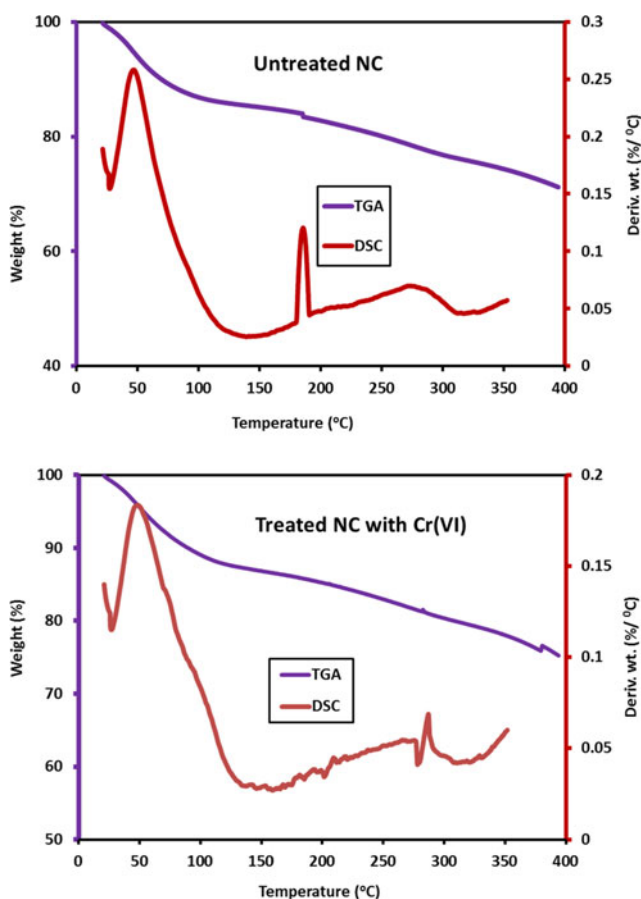


**Fig. 5** TGA and DSC of NC and NC treated with Cr(VI)

treated with Cr (VI) can be attributed to loss of adsorbed moisture. The weight loss from  $\sim 148$  to  $\sim 268$  °C in untreated NC and from  $\sim 155$  to  $\sim 308$  °C in treated NC with Cr(VI) is due to the elimination of the HCl dopant. The last step of weight loss over  $\sim 279$  and  $\sim 320$  °C for untreated NC and NC treated with Cr(VI), respectively, is due to the degradation of PANI chains [23–25]. This similarity in the mass loss is an evidence of the stability of treated NC. The DSC thermographs of untreated and treated NC present exothermic peaks at about 50, 180, and 270 °C. These peaks are attributed to glass transition temperature (T<sub>g</sub>), dedoping, and degradation of PANI, respectively.

### Effect of different conditions on removal percentage and capacity of Cr(VI)

#### Effect of pH

The effect of pH of the Cr(VI) solutions was investigated as one of the most important parameters controlling their adsorption onto NC. It is indicated that pH of the solution influences the chemical speciation of the Cr ions as well as the ionization of the functional groups onto the adsorbent NC surfaces. In

addition, pH affects the surface charge characteristics of the adsorbents. Effect of pH on both  $R$  and  $Q$  for Cr(VI) solutions after treatment with 0.4 g/L of NC for 6 min at room temperature is illustrated in Fig. 6. Cr(VI) ions are detoxified with 99.2 % at pH 2.0. A decrease of the Cr(VI) removal with about 63.6 % is observed in the solution of pH 11.0 whereas a slight decreasing of the Cr(VI) removal percentages is observed in the range of pH from 2.0 to 9.0. This confirmed that PANI salt in the NC is dedoped and deprotonated at high pH. This is indicated that the synthesized NC is suitable for Cr(VI) removal over a wide pH range. These results are in agreement with the results obtained by Gu et al. [10] and Guo et al. [26]. The  $Q$  value has the same tendency of  $R$ , and the maximum  $Q$  value of 17.36 mg/g is obtained pH 2.0. Then  $Q$  is decreased again to 11.14 mg/g at pH 11.0.

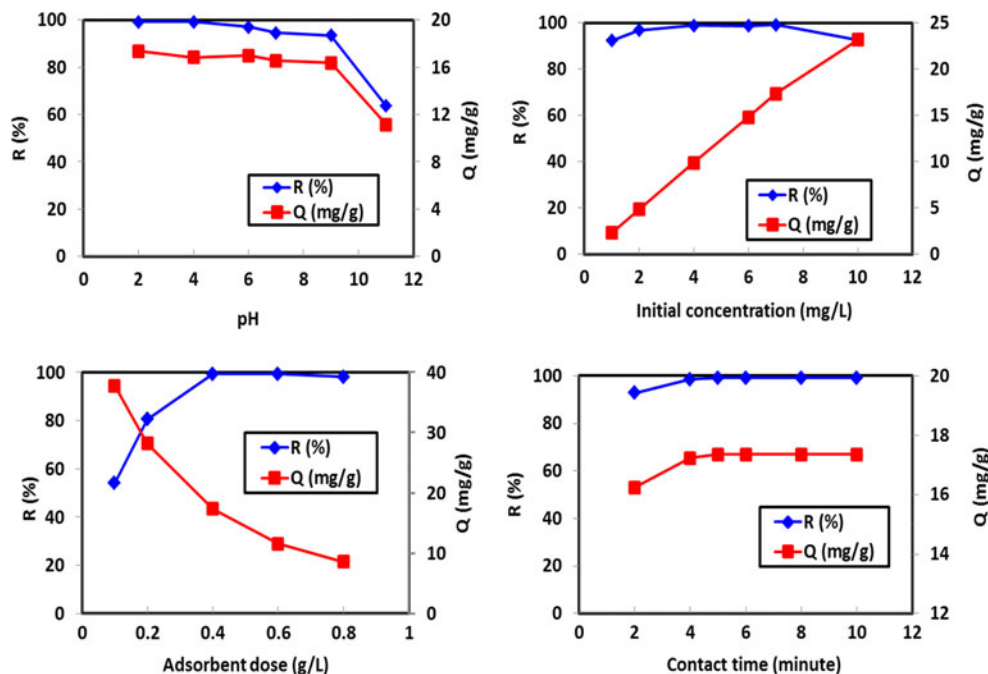
#### Effect of initial Cr(VI) concentration

The effect of initial Cr(VI) concentration on the  $R$  and  $Q$  is investigated at pH 2.0 by using 0.4 g/L of NC as shown in Fig. 6. It is cleared that increasing of the Cr(VI) concentration, the  $R$  is slightly increased. Then, it is attained a maximal value of nearly 99.2 % at Cr(VI) concentration of 7.0 mg/L. This is may be due to availability of the adsorption sites which initially leads to the increase in the Cr(VI) adsorption [27]. The decline in the removal percentage at higher concentrations of Cr(VI) may be due to nonavailability of adsorbent surface [1]. Moreover, the oxidation and degradation of polyaniline can be raised at oxidative environment of the concentrated Cr(VI) ions [10, 28]. It is found that  $Q$  has linearly increased with the increase of the initial concentration of Cr(VI). The increment of initial concentration of Cr(VI) provides a driving force to overcome the mass transfer resistance of Cr(VI) ions between the aqueous and solid phases and resulting in a higher probability of collision between Cr(VI) ions and NC adsorbent [29].

#### Effect of PANI/akaganéite nanocomposite adsorbent dose

To evaluate the optimum dose of NC, the effect of the synthesized dose on Cr(VI)  $R$  and  $Q$  is studied at pH 2.0 in 25 ml of 7.0 mg/L Cr(VI) solution for 6 min as indicated in Fig. 6. The  $R$  is observed to increase with increasing the NC dose. This is likely due to an increase in the surface area and availability of more adsorbent sites [29]. For low range of NC dose  $< 0.4$  g/L, the  $R$  of Cr(VI) is linearly increased. The maximum  $R$  is obtained at 0.4 g/L, and further increase in the NC doses does not increase the  $R$ . This suggested that after a certain dose of NC adsorbent, the maximum removal is attained and hence the amount of ions are bound to the adsorbent, and the amount of free ions remain constant even with further addition of the dose of adsorbent [27]. On the other hand, the  $Q$  of Cr(VI) is decreased with increasing the NC dose from 0.1 to 0.8 g/L.

**Fig. 6**  $R$  and  $Q$  versus pH, initial Cr(VI) concentration, adsorbent dose, and contact time in 25 ml Cr(VI) solution



This may be attributed to the formation of aggregates that would reduce the availability of effective sorption area, hence decreasing the overall metal capacity [30].

#### Effect of contact time

The contact time between metal ions and adsorbents helps in identifying the possible speed of binding and removal of Cr(VI) ions and also evaluating the optimum time for maximum removal. It is substantial that the NC adsorbent offers rapid removal kinetics for efficient adsorbate removal from solution. Figure 6 presents the effect of contact time between NC and Cr(VI) on the  $R$  and  $Q$  of 7.0 mg/L Cr(VI) solutions. After 2 min of the contact time, high  $R$  value of 92.8 % is obtained. As contact time increases, the removal efficiency of Cr(VI) ions by the NC is increased due to the availability of abundant active sites on the nanocomposite surface. At about 5 min, the equilibrium reaction time between the Cr(VI) ions and NC exhibits the maximum  $R$ . The optimum contact time to remove about 99 % of the Cr(VI) ions is 5 min for the NC which is short compared to the equilibrium time using other materials. The polyaniline powder has been reported to require contact time of 10–12 min [31], activated carbon requires contact time of 3 h [32], polypyrrole/Fe<sub>3</sub>O<sub>4</sub> magnetic nanocomposites require contact time of 30 min [33], oxidized multiwalled carbon nanotubes require contact time of 280 min [34], and nanocrystalline akaganéite requires contact time of 1 h [35]. The  $Q$  is observed to increase from 16.5 to 17.5 mg/g by increasing the contact time from 2 to 5 min.  $Q$  is increased with the increase of the contact time until the equilibrium is

established between the solid phase and liquid phase in the adsorption system [2, 36].

#### Effect of adsorbent type

The  $R$  and  $Q$  values are compared and investigated using different adsorbents. These adsorbents are NC, akaganéite NPs, and PANI salt. Doses of 0.4 g/L of each adsorbent were used to treat 25 ml solutions of an initial Cr(VI) concentration of 7.0 mg/L at pH 2.0 and pH 11.0 for 6 min at room temperature as shown in Table 1. The comparable study of NC, akaganéite NPs, and PANI towards the Cr(VI) removal indicates that these adsorbents are efficiently able to remove Cr(VI) at the optimum pH 2.0. However, NC is more favorable as adsorbents for Cr(VI) removal than PANI and akaganéite NPs because PANI and akaganéite NPs show lower removal efficiencies especially under alkaline condition. Polyaniline powder is generally aggregated in the solution and missing the advantage of the magnetically separation. In addition, iron-oxide NPs shows poor stability under acidic conditions [37].

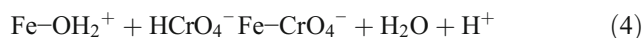
**Table 1**  $R$  of Cr(VI) solutions (7.0 mg/L) using different adsorbents at pH 2.0 and pH 11.0 after 6 min

pH Adsorbent (0.4 g/L)	pH 2 (R %)	pH 11 (R %)
NC	99.2	63.6
Akaganéite NPs	90.9	2.2
PANI	86.0	42.5



*Mechanism of removal Cr(VI) ions using PANI/akaganéite nanocomposite*

Cr(VI) ions can be existed in solution with different ionic forms depending on pH.  $\text{HCrO}_4^-$  is the dominant ion at pH lower than 6.8, and  $\text{CrO}_4^{2-}$  is the dominant at pH above 6.8 [2]. There are two proposed mechanisms describing the removal of Cr(VI) by the prepared NC. In the first mechanism, the ion exchange occurred between the dopant ( $\text{Cl}^-$ ) and the monovalent bichromate ( $\text{HCrO}_4^-$ ) ions in the solutions with low pH according to Bhaumik et al. [38]. Also, the electron-donating groups onto polyaniline exist in the nanocomposite reduce the Cr(VI) species to Cr(III) species. Meanwhile, the polyaniline layer is partially converted into its oxidized state after treatment with Cr(VI). The oxidation of polyaniline and reduction of Cr(VI) is shown in Fig. 7. For the second mechanism, the direct reduction of Cr(VI) to Cr(III) ions occurs and follows by partial adsorption for Cr(III) as indicated in Fig. 7. In the case of protonated imine nitrogens in emeraldine salt (PANI-ES),  $\text{H}^+$  ion-exchange with Cr(III) can lead to Cr(III) adsorption on PANI backbone [28]. In addition, the surface complexation reactions for Cr(VI) ions and akaganéite may be written as the following equations [35]:



pH value determines the surface charge of akaganéite NPs; therefore, the high removal efficiency at low pH can be attributed to the fact that the surface of the NC becomes highly protonated and positively charged, which favors the uptake of Cr(VI) anions through electrostatic attraction. An increase in the solution pH will make the surface negatively charged, greatly weakening the electrostatic attraction between NC and negatively charged Cr(VI) anions, thus reducing the removal efficiency. Moreover, as the pH increases, there is competition between  $\text{OH}^-$  in the solution and chromate ( $\text{CrO}_4^{2-}$ ) ions for the available adsorption sites on the NC surface [36, 39]. These mechanisms are in agreement with the other work [2, 40].

*Removal of Cr(VI) ions from wastewater sample*

It is essential to investigate the potential application of the NC for the removal of Cr(VI) ions from wastewater sample. An industrial wastewater sample of a leather tanning company contaminated with 0.6 mg/L and spiked with 6.0 mg/L to have 6.6 mg/L of Cr(VI) ions was selected to accomplish this study. The spiked wastewater sample is studied for the removal of Cr(VI) ions by mixing 25 ml of this sample with 10.0 mg (0.4 g/L) of NC at pH 2.0 and pH 7.2 (pH of the wastewater sample) for 6 min at room temperature. Results reveal that NC is able to remove about 93.4 % of Cr(VI) ions at pH 2.0 and 52.5 % at pH 7.2. These data confirm the high ability of the synthesized NC for the removal of Cr(VI) by simple controlling and monitoring of the pH value of wastewater.

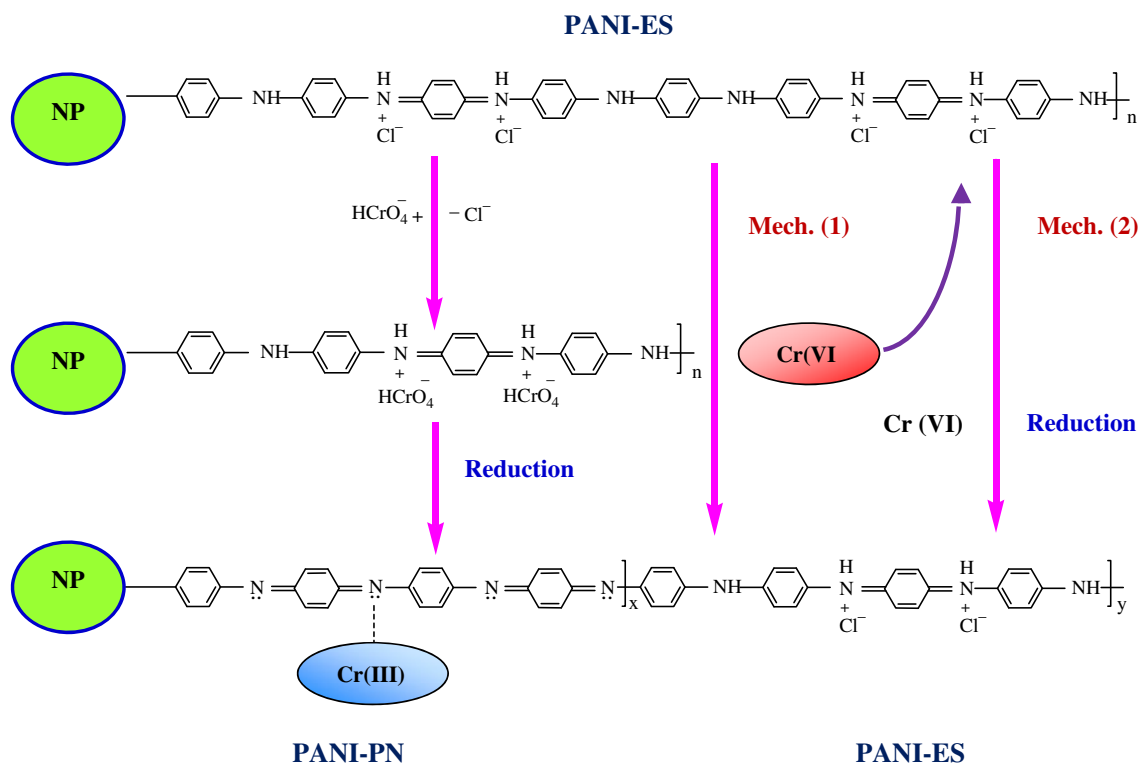


Fig. 7 Proposed removal mechanism of PANI

## Conclusions

PANI/akaganéite nanocomposite was synthesized, characterized, and applied as an effective adsorbent for the removal of Cr(VI) from aqueous solution. This nanocomposite was rapidly and efficiently removed Cr(VI) from aqueous solution with a wide pH range. It was found that the electron diffraction pattern of the prepared nanocomposite is a polycrystalline material with an average d-spacing of 2.78 nm. The results indicated that removal efficiency was highly pH dependent and 99.2 % removal was obtained at pH 2.0, 7.0 mg/L of Cr(VI) and 0.4 g/L NC dose after 5 min. The NC was successfully removed Cr(VI) from a leather tanning wastewater sample with 93.4 % efficiency at pH 2.0.

## References

- Karthik R, Meenakshi S (2014) Removal of hexavalent chromium ions using polyaniline/silica gel composite. *J Water Process Eng* 1: 37–45
- Tang L, Fang Y, Pang Y, Zeng G, Wang J, Zhou Y, Deng Y, Yang G, Cai Y, Chen J (2014) Synergistic adsorption and reduction of hexavalent chromium using highly uniform polyaniline-magnetic mesoporous silica composite. *Chem Eng J* 254:302–312
- Zhu J, Wei S, Gu H, Rapole SB, Wang Q, Luo Z, Haldolaarachchige N, Young DP, Guo Z (2012) One-pot synthesis of magnetic graphene nanocomposites decorated with Core@Double-shell nanoparticles for fast chromium removal. *Environ Sci Tech* 46: 977–985
- Ebrahim SM, Kashyout AB, Soliman MM (2007) Electrical and structural properties of polyaniline/cellulose triacetate blend films. *J Polym Res* 14(5):423–429
- Wang J, Zhang K, Zhao L (2014) Sono-assisted synthesis of nanostructured polyaniline for adsorption of aqueous Cr(VI): Effect of protonic acids. *Chem Eng J* 239:123–131
- Ebrahim S, El-Raey R, Hefnawy A, Ibrahim H, Soliman M (2014) Electrochemical sensor based on polyaniline nanofibers/single wallcarbon nanotubes composite for detection of malathion. *Synth Met* 190:13–19
- Adegoke HI, Adekola FA, Fatoki OS, Ximba BJ (2014) Adsorption of Cr(VI) on synthetic hematite ( $\alpha$ -Fe<sub>2</sub>O<sub>3</sub>) nanoparticles of different morphologies. *Korean J Chem Eng* 31(1):142–154
- Zhang YX, Jia Y (2014) A facile solution approach for the synthesis of akaganéite ( $\beta$ -FeOOH) nanorods and their ion-exchange mechanism toward As(V) ions. *Appl Surf Sci* 290:102–106
- Kumari M, Pittman CU, Mohan D (2015) Heavy metals [chromium (VI) and lead(II)] removal from water using mesoporous magnetite (Fe<sub>3</sub>O<sub>4</sub>) nanospheres. *J Colloid Interface Sci* 442:120–132
- Gu H, Rapole SB, Sharma J, Huang Y, Cao D, Colorado HA, Luo Z, Haldolaarachchige N, Young DP, Walters B, Wei S, Guo Z (2012) Magnetic polyaniline nanocomposites toward toxic hexavalent chromium removal. *RSC Adv* 2:11007–11018
- Han X, Gai L, Jiang H, Zhao L, Liu H, Zhang W (2013) Core-shell structured Fe<sub>3</sub>O<sub>4</sub>/PANI microspheres and their Cr(VI) ion removal properties. *Synth Met* 171:1–6
- Li R, Liu L, Yang F (2013) A study on the reduction behaviors of Cr(VI) on Fe<sub>3</sub>O<sub>4</sub>/PANI. *Procedia Environ Sci* 18:522–527
- Rezvani M, Asgharinezhad AA, Ebrahimzadeh H, Shekari N (2014) A polyaniline-magnetite nanocomposite as anion exchange sorbent for solid phase extraction of chromium (VI) ions. *Microchim Acta* 181:1887–1895
- Zhao J, Lin W, Chang Q, Li W, Lai Y (2012) Adsorptive characteristics of akaganéite and its environmental applications: a review. *Environ Technol Rev* 1(1):114–126
- Gomes EC, Oliveira MS (2012) Chemical polymerization of aniline in hydrochloric acid (HCl) and formic acid (HCOOH) media. Differences between the two synthesized polyanilines. *American J Polm Sci* 2:5–13
- Jiang N, Xu Y, Dai Y, Luo W, Dai L (2012) Polyaniline nanofibers assembled on alginate microsphere for Cu<sup>2+</sup> and Pb<sup>2+</sup> uptake. *J Hazard Mater* 215:17–24
- Najim TS, Salim AJ (2014) Polyaniline nanofibers and nanocomposites: Preparation, characterization, and application for Cr(VI) and phosphate ions removal from aqueous solution. *Arabian J Chem*. doi:10.1016/j.arabjc.2014.02.008
- Ullah R, Deb BK, Mollah MA (2014) Synthesis and characterization of silica coated iron-oxide composites of different ratios. *Int J Compos Mater* 4:135–145
- Gu H, Huang Y, Zhang X, Wang Q, Zhu J, Shao L, Haldolaarachchige N, Young DP, Wei S, Guo Z (2012) Magneto-resistive polyaniline-magnetite nanocomposites with negative dielectrical properties. *Polymer* 53:801–809
- Wen T, Fan Q, Tan X, Chen Y, Chen C, Xu A, Wang X (2016) A core-shell structure of polyaniline coated protonic titanate nanobelt composites for both Cr(VI) and humic acid removal. *Polym Chem* 7:785–794
- Mostafaei A, Zolriasatein A (2012) Synthesis and characterization of conducting polyaniline nanocomposites containing ZnO nanorods. *Prog Nat Sci Mat Int* 22:273–280
- Bhaumik M, Setshedi K, Maity A (2013) Chromium (VI) removal from water using fixed bed column of polypyrrole/Fe<sub>3</sub>O<sub>4</sub> nanocomposite. *Sep Purif Technol* 110:11–19
- Zhang S, Zeng M, Xu W, Li J, Li J, Xu J, Wang X (2013) Polyaniline nanorods dotted on graphene oxide nanosheets as a novel super adsorbent for Cr(VI). *Dalton Trans*. doi: 10.1039/c3dt50149c
- Shao D, Hou G, Li J, Wen T, Ren X, Wang X (2014) PANI/GO as a Super Adsorbent for the Selective Adsorption of Uranium(VI). *Chem Eng J*, doi: <http://dx.doi.org/10.1016/j.cej.2014.06.063>
- Ren G, Qiu H, Wu Q, Li H, Fan H, Fang C (2010) Thermal stability of composites containing HCl-doped polyaniline and Fe nanoparticles. *Mater Chem Phys* 120:127–133
- Guo X, Fei GT, Su H, Zhang LD (2011) High-performance and reproducible polyaniline nanowire/tubes for removal of Cr(VI) in aqueous solution. *J Phys Chem C* 115:1608–1613
- Pandey S, Mishra SB (2011) Organic-inorganic hybrid of chitosan/organoclay bionanocomposites for hexavalent chromium uptake. *J Colloid Interf Sci* 361:509–520
- Krishnani KK, Srinives S, Mohapatra BC, Boddu VM, Hao J, Meng X, Mulchandani A (2013) Hexavalent chromium removal mechanism using conducting polymers. *J Hazard Mater* 252–253: 99–106
- Mthombeni NH, Onyango MS, Aoyi O (2015) Adsorption of hexavalent chromium onto magnetic natural zeolite-polymer composite. *J Taiwan Inst Eng* 50:242–251
- Yong-Mei H, Man C, Zhong-Bo H (2010) Effective removal of Cu(II) ions from aqueous solution by amino-functionalized magnetic nanoparticles. *J Hazard Mater* 184:392–399
- Olad A, Nabavi R (2007) Application of polyaniline for the reduction of toxic Cr(VI) in water. *J Hazard Mater* 147:845–851
- Babel S, Kurniawan TA (2004) Cr (VI) removal from synthetic wastewater using coconut shell charcoal and commercial activated carbon modified with oxidizing agents and/or chitosan. *Chemosphere* 54:951–967

33. Bhaumik M, Maity A, Srinivasu VV, Onyango MS (2011) Enhanced removal of Cr(VI) from aqueous solution using polypyrrole/Fe<sub>3</sub>O<sub>4</sub> magnetic nanocomposite. *J Hazard Mater* 190:381–390
34. Hu J, Chen C, Zhu X, Wang X (2009) Removal of chromium from aqueous solution by using oxidized multiwalled carbon nanotubes. *J Hazard Mater* 162:1542–1550
35. Lazaridis NK, Bakoyannakis DN, Deliyanni EA (2005) Chromium(VI) sorptive removal from aqueous solutions by nanocrystalline akaganéite. *Chemosphere* 58:65–73
36. Tang L, Yang GD, Zeng GM, Cai Y, Li SS, Zhou YY, Pang Y, Liu YY, Zhang Y, Luna B (2014) Synergistic effect of iron doped ordered mesoporous carbon on adsorption-coupled reduction of hexavalent chromium and the relative mechanism study. *Chem Eng J* 239:114–122
37. Liu Y, Chen M, Hao Y (2013) Study on the adsorption of Cu(II) by EDTA functionalized Fe<sub>3</sub>O<sub>4</sub> magnetic nano-particles. *Chem Eng J* 218:46–54
38. Bhaumik MC, Hyung J, McCrindle RI, Maity A (2014) Composite nanofibers prepared from metallic iron nanoparticles and polyaniline: high performance for water treatment applications. *J Colloid Interface Sci* 425:75–82
39. Jabeen H, Chandra V, Jung S, Lee JW, Kim SK, Kim SB (2011) Enhanced Cr(VI) removal using iron nanoparticle decorated grapheme. *Nanoscale* 3:3583–3585
40. Xu H, Zhang H, Lv T, Wei H, Song F (2013) Study on Fe<sub>3</sub>O<sub>4</sub>/ polyaniline electromagnetic composite hollow spheres prepared against sulfonated polystyrene colloid template. *Colloid Polym Sci* 291:1713–1720